



**HAL**  
open science

## Relief Extraction of Rough Textured Reflecting Surface by Image Processing

Xin Huang, Jacques Brochard, David Helbert, Majdi Koudeir

► **To cite this version:**

Xin Huang, Jacques Brochard, David Helbert, Majdi Koudeir. Relief Extraction of Rough Textured Reflecting Surface by Image Processing. Eighth International Conference on Quality Control by Artificial Vision 2007, May 2007, Le Creusot, France. [http://spie.org/x648.xml?product\\_id=736719&Search\\_Origin=QuickSearch&Search\\_Results\\_URL=http://10.1117/12.736719](http://spie.org/x648.xml?product_id=736719&Search_Origin=QuickSearch&Search_Results_URL=http://10.1117/12.736719) . hal-00331499

**HAL Id: hal-00331499**

**<https://hal.science/hal-00331499>**

Submitted on 4 Apr 2023

**HAL** is a multi-disciplinary open access archive for the deposit and dissemination of scientific research documents, whether they are published or not. The documents may come from teaching and research institutions in France or abroad, or from public or private research centers.

L'archive ouverte pluridisciplinaire **HAL**, est destinée au dépôt et à la diffusion de documents scientifiques de niveau recherche, publiés ou non, émanant des établissements d'enseignement et de recherche français ou étrangers, des laboratoires publics ou privés.

# Relief Extraction of Rough Textured Reflecting Surface by Image Processing

Xin Huang, Jacques Brochard, David Helbert and Majdi Khoudeir

SIC Laboratory (E.A. 4103), University of Poitiers, 86962 Futuroscope-Chasseneuil Cedex, France.

## 1. INTRODUCTION

In this paper, we present a method for relief extraction of rough textured reflecting surface by image processing. The rough textured reflecting surface is the surface which mixes both diffuse and specular components.

Rough surface relief extraction is generally made by a mechanical method using a tactile sensor or by using an auto-focus laser sensor. With these sensors we can estimate surface relief from the analysis of a series of profiles. Since these measurements spend a lot of time, we hope that we can determine the relief by image processing. Several methods in the field of image processing have been proposed for relief extraction, such as shape from shading<sup>1</sup>, optical flow<sup>2</sup>, shape from focus<sup>3</sup> and photometric stereovision<sup>4</sup>. Our works are based on the photometric stereovision. In 1980, Woodham indicated that the relief of a Lambertian surface can be determined by the exploitation of a photometric model, which takes into account camera and light source positions according to the plan of surface.<sup>4</sup> The proposed model expresses the gray level on the image according to the local relief variations. Three images of the same relief obtained under different angles of lighting are used to reconstruct the surface relief. From the method of Woodham, several important ameliorations have been proposed by other researchers.<sup>5-7</sup> But a limit study in section 2.1.3 proves that the above methods worked with Lambert's model is adapted to the diffuse reflection, but not to the specular reflection.

Thus, we propose another method to extract the relief of rough textured reflecting surface. In the proposed method, we show that the diffuse and specular components of the acquired images can be decomposed in two independent components. The diffuse component can be processed by Lambert's model, the specular component can be processed according to the position knowledge of facets. Finally, section 3 presents the experimental results obtained by this method, and compares measurement precision with the experimental results obtained by Lambert's model.

## 2. RELIEF EXTRACTION BY PHOTOMETRIC STEREOVISION

Relief extraction can be obtained by photometric stereovision. In this section, we will clarify how to establish the photometric stereovision system from the exploitation of several photometric models and study the performance of these photometric stereovision systems for rough textured reflecting surface.

### 2.1. Lambert's model

#### 2.1.1. Relation between gray level and relief variations

To establish the link between the gray level variations and those of relief, we can use the Lambert's model which is the most common model for describing the diffuse reflection. Lambert's model states that the incidence light on a surface is scattered equally in all directions;<sup>8</sup> the total amount of reflected light depends on the lighting incidence angle.

---

Further author information: (Send correspondence to David Helbert)

Xin Huang: E-mail: huang@sic.univ-poitiers.fr, Telephone: (+33) 549 496 572

Jacques Brochard: E-mail: brochard@sic.univ-poitiers.fr, Telephone: (+33) 549 496 611

David Helbert: E-mail: helbert@sic.univ-poitiers.fr, Telephone: (+33) 549 496 580

Majdi Khoudeir: E-mail: khoudeir@sic.univ-poitiers.fr, Telephone: (+33) 549 496 593

This means that the gray level depends on the lighting incidence angle of facet, so the problem is that we must find out the link between this angle and the surface relief. Fortunately, according to the position knowledge of source and the camera in figure 1, we can find out the link between this angle and the surface gradient field  $\{p = \frac{\partial z}{\partial x}, q = \frac{\partial z}{\partial y}\}$ , then the link between the gray level (intensity received  $E(x, y)$ ) and the gradient field  $\{p, q\}$ :

$$E(x, y) = \rho \frac{I_0 \cos \theta - p \sin \theta \cos \varphi_i - q \sin \theta \sin \varphi_i}{\sqrt{1 + p^2 + q^2}} \quad (1)$$

where  $\rho$  is the surface albedo,  $I_0$  the light source intensity,  $r$  the distance between light source and facet,  $\theta$  the angle between lighting direction and surface normal,  $\varphi_i$  the azimuth angles between  $\vec{x}$  axis and the projection of three sources in the  $(\vec{x}, \vec{y})$  plane.

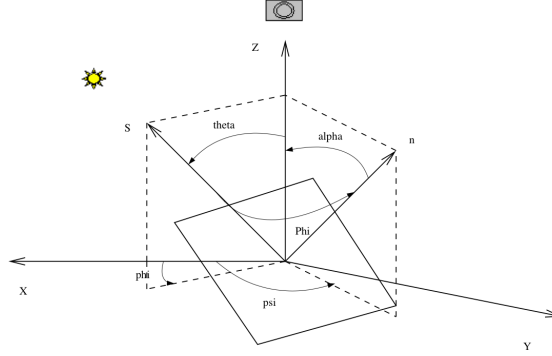


**Figure 1.** Illumination received by the sensor.

### 2.1.2. Relief extraction

In equation 1, we have three unknown parameters  $p, q, \rho \frac{I_0}{r^2}$ . We thus need to acquire three images of the studied surface under different angles of lighting to establish an equations set ( $\varphi_1 = \pi, \varphi_2 = \frac{\pi}{3}$  and  $\varphi_3 = -\frac{\pi}{3}$ ). After resolving this equation set, we determine  $p$  and  $q$ :

$$p = \frac{2 - \left(\frac{E_3}{E_1}\right) - \left(\frac{E_2}{E_1}\right)}{\tan \theta \left[1 + \left(\frac{E_2}{E_1}\right) + \left(\frac{E_3}{E_1}\right)\right]} \quad (2)$$

$$q = \frac{\sqrt{3} \left(\frac{E_3}{E_1}\right) - \left(\frac{E_2}{E_1}\right)}{\tan \theta \left[1 + \left(\frac{E_2}{E_1}\right) + \left(\frac{E_3}{E_1}\right)\right]} \quad (3)$$

It exists various algorithm to obtain a 3D reconstruction from the gradient field  $\{p, q\}$  of a surface.<sup>1,9,10</sup> In this paper, we use the algorithm of Frankot and Chellappa<sup>11</sup> which proposes a method to reconstruct the surface  $z = f(x, y)$  by minimizing the following cost function:

$$W = \int \int \left( \left( -\frac{\partial f(x, y)}{\partial x} \right) - p \right)^2 + \left( \left( -\frac{\partial f(x, y)}{\partial y} \right) - q \right)^2 dx dy \quad (4)$$

With the theorem of Parseval, the cost function becomes:

$$W = \frac{1}{2\pi} \int \int \left| -ju\tilde{f}(u, v) - \tilde{p} \right|^2 + \left| -jv\tilde{f}(u, v) - \tilde{q} \right|^2 dudv \quad (5)$$

where  $\tilde{f}(u, v)$  is the Fourier Transform of the function  $f(x, y)$ ,  $\tilde{p}$  and  $\tilde{q}$  are the Fourier Transform of the gradient field  $\{p, q\}$ . After minimization of this expression, we determine a relation between the Fourier Transform of the

surface and the Fourier Transform of the gradient field:

$$\tilde{f}(u, v) = \frac{-ju\tilde{p}^* - jv\tilde{q}^*}{u^2 + v^2} \quad (6)$$

Consequently, the reconstructed surface  $z = f(x, y)$  can be obtained by Inverse Fourier Transform of  $\tilde{f}(u, v)$ .

### 2.1.3. Limits of the classical approach

As we know in<sup>4</sup>, the above classical photometric stereovision technique of Lambert's model was exploited for rough textured surface. So, we will study whether this technique is adapted to rough textured reflecting surface through experiment. We acquire three images of a real cylinder (See figure 2). The reason we study a columned object is that all slope is presented on a cylinder. We find several specular areas in the images 2, 3, so this cylinder surface mixes both diffuse and specular components. Through Lambert's model, we extract the relief of the cylinder (See figure 3(a)) and the associated profiles which consists of diffuse and specular components (See figure 3(b)). We find also a specular area in figure 3(a), this specular area appears in figure 3(b) as a convexity in the center of the figure.

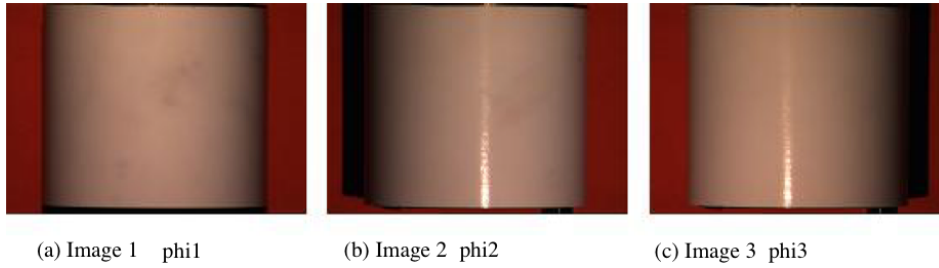


Figure 2. Three acquired images.

Thus, the method by Lambert's model do not eliminate the influence of specular reflection and it do not reconstruct the cylinder surface perfectly. We then focus our attention on other model for specular reflection.

### 2.2. Model for specular reflection

In the case of specular reflection, the reflected ray is visible only when the reflected direction and the view direction coincide. But in fact the situation is rarely so simple that the reflected ray can be seen even if these two directions do not coincide. Phong proposed his model<sup>12</sup> which depends on the angle between the specular direction and the view direction:

$$E(x, y) = \rho \frac{I_0}{r^2} \cos i (\cos \alpha)^n \quad (7)$$

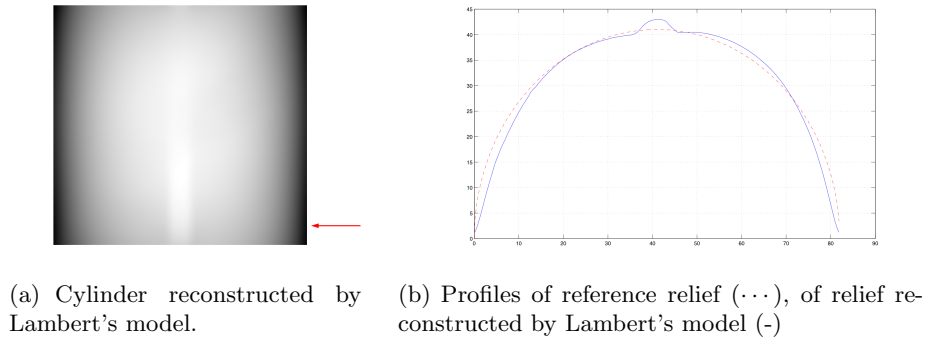
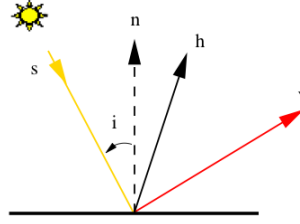


Figure 3. Cylinder and profile reconstructed.

where  $n$  is the specular coefficient and  $\alpha$  the angle between specular direction and view direction. The specular coefficient  $n$  depends on the surface nature and it requires to be estimated.

Blinn came up with an alternative way to calculate the specular reflection, which eliminates the expensive reflection vector calculations<sup>13</sup>. To do this, Blinn introduced the half vector  $\vec{h}$ , which is a vector halfway between the light vector and the view vector ( $\vec{h} = (\vec{s} + \vec{v})/|\vec{s} + \vec{v}|$ ) (See figure 4). Blinn proved that we can optimize the Phong model by using  $\cos(\vec{n}, \vec{h})$  instead of  $\cos \alpha$ :

$$E(x, y) = \rho \frac{I_0}{r^2} \cos^i(\cos(\vec{n}, \vec{h}))^n \quad (8)$$



**Figure 4.** Case of Blinn-phong model.

However, in this two photometric models, we do not know the value of specular coefficient  $n$ . So it's very difficult to determine the gradient field  $\{p, q\}$  through these models. Then we hope to find another way to extract the relief of rough textured reflecting surface more simply.

## 2.3. The suggested approach

### 2.3.1. Gradient field of specular area

In the proposed method, to extract the relief of the surface mixing diffuse and specular components, we decompose the acquired images in two terms, a diffuse component and a specular component. The diffuse component can be processed by Lambert's model. The specular component can be processed according to the position knowledge of facets.

The idea is to detect first the specular area on the image and then to compute the corresponding local gradient by using the light source and camera positions. We thus obtain the gradient value, through Lambert's model, for the diffuse region of the surface, and the gradient value for the specular region is obtained by the suggested method. The global gradient field is then integrated to extract the relief of the surface.

We suppose that a pixel is specular when its gray level is more superior than a threshold. We can extend this supposition to entire image and find the specular area. Figure 5 illustrates the decomposition procedure.

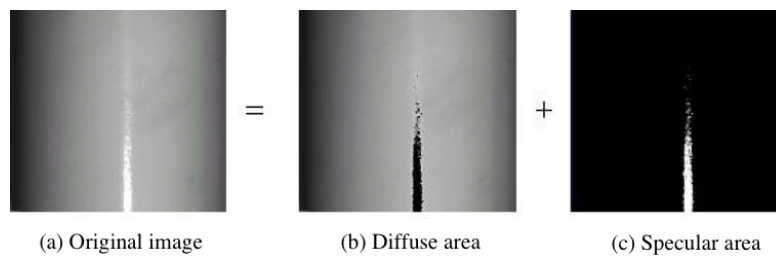


**Figure 5.** Image decomposition

### 2.3.2. Gradient computation

The computation of gradient field  $\{p_d, q_d\}$  of diffuse area can be executed by the method of Lambert's model (equations 2, 3). Then we present the computation of gradient field  $\{p_s, q_s\}$  of specular area according to the position knowledge of facets.

In the specular facet, we can find that the half vector  $\vec{h}$  coincides with the facet normal  $\vec{n}$  because the view direction coincides with the reflected direction. So according to the property of half vector, we obtain:

$$\vec{n} = \vec{h} = \frac{\vec{s} + \vec{v}}{|\vec{s} + \vec{v}|} = \frac{\vec{s} + \vec{v}}{\sqrt{2 + 2 \cos(\vec{s}, \vec{v})}} = \frac{\vec{s} + \vec{v}}{2 \cos \frac{\vec{s}, \vec{v}}{2}} \quad (9)$$

The camera direction is perpendicular ( $\vec{v} = \vec{z} = \begin{bmatrix} 0 \\ 0 \\ 1 \end{bmatrix}$  and  $\vec{z}$  is the normal of the surface), we thus obtain:

$$\vec{n} = \frac{\vec{s} + \vec{z}}{2 \cos \frac{\vec{s}, \vec{z}}{2}} = \frac{\vec{s} + \vec{z}}{2 \cos \frac{\theta}{2}} \quad (10)$$

From light source position and facet normal position in figure 3 we know that:

$$\vec{s} = \begin{bmatrix} \sin \theta \cos \varphi_i \\ \sin \theta \sin \varphi_i \\ \cos \theta \end{bmatrix}, \quad \vec{n} = \frac{1}{\sqrt{1 + p^2 + q^2}} \begin{bmatrix} -p \\ -q \\ 1 \end{bmatrix}$$

So,

- Specular area on image 1 ( $\varphi_1 = \pi$ ):

$$\vec{s}_1 = \begin{bmatrix} \sin \theta \cos \pi \\ \sin \theta \sin \pi \\ \cos \theta \end{bmatrix} = \begin{bmatrix} -\sin \theta \\ 0 \\ \cos \theta \end{bmatrix} \quad (11)$$

$$\vec{n} = \frac{\vec{s}_1 + \vec{z}}{2 \cos \frac{\theta}{2}} = \frac{1}{2 \cos \frac{\theta}{2}} \begin{bmatrix} -\sin \theta \\ 0 \\ 1 + \cos \theta \end{bmatrix} = \frac{1}{\sqrt{1 + p^2 + q^2}} \begin{bmatrix} -p \\ -q \\ 1 \end{bmatrix} \quad (12)$$

After solving this expression:

$$\begin{cases} p_1 = \frac{\sin \theta}{1 + \cos \theta} \\ q_1 = 0 \end{cases} \quad (13)$$

In the same way, we can find the gradients of the specular area of other images.

- Specular area on image 2 ( $\varphi_2 = \pi/3$ ),

$$\begin{cases} p_2 = -\frac{1}{2} \frac{\sin \theta}{1 + \cos \theta} \\ q_2 = -\frac{\sqrt{3}}{2} \frac{\sin \theta}{1 + \cos \theta} \end{cases} \quad (14)$$

- Specular area on image 3 ( $\varphi_3 = -\pi/3$ ),

$$\begin{cases} p_3 = -\frac{1}{2} \frac{\sin \theta}{1 + \cos \theta} \\ q_3 = \frac{\sqrt{3}}{2} \frac{\sin \theta}{1 + \cos \theta} \end{cases} \quad (15)$$

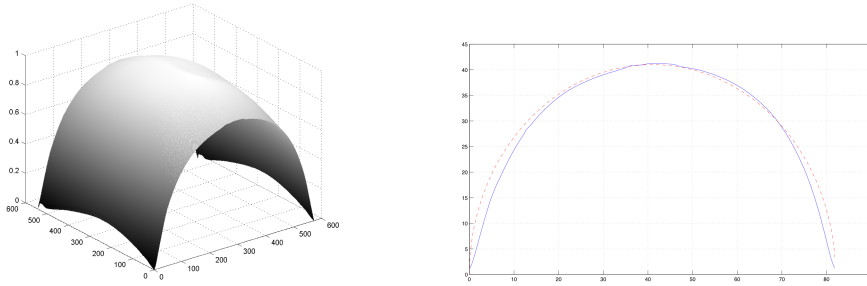
Since the specular areas of three images are disjoint, the gradient field of specular area on every image can compose the gradient field  $\{p_s, q_s\}$  of specular area on surface.

### 2.3.3. Relief extraction

We have previously determined the gradient field  $\{p_d, q_d\}$  of diffuse area and the gradient field  $\{p_s, q_s\}$  of specular area on the same surface. Then the gradient field  $\{p, q\}$  consisted of the gradient field  $\{p_d, q_d\}$  of diffuse area and the gradient field  $\{p_s, q_s\}$  of specular area can be used for relief extraction through the algorithm of section 2.1.2.

## 3. EXPERIMENTAL RESULTS

In order to realize the method of relief extraction, we exploited an acquisition system. In this system, we use respectively three light sources to illuminate an object from three different angles ( $\varphi_1 = -\pi$ ,  $\varphi_2 = \frac{\pi}{3}$  and  $\varphi_3 = -\frac{\pi}{3}$ ), and we acquire respectively three images in perpendicular direction by using a camera. With this system, we have acquired three images of a real cylinder (See figure 2) of size  $540 \times 570$ . In order to reconstruct this cylinder surface more perfectly than Lambert's model, we extract the relief (See figure 6(a)) and a profile (See figure 6(b)) by the proposed method. Obviously, the specular area does not exist in figure 6(a) and 6(b).



(a) Cylinder reconstructed by the proposed method. (b) Profiles of reference relief ( $\cdots$ ), of relief reconstructed by the proposed method ( $-$ ).

**Figure 6.** Cylinder and profile reconstructed.

We propose the error coefficient  $C_e$  (equation 16) to compare the measurement precision:

$$C_e = \frac{\sum_{x=1}^N \sum_{y=1}^M |Z_{x,y} - z_{x,y}|}{\sum_{x=1}^N \sum_{y=1}^M |Z_{x,y}|} \quad (16)$$

Where  $Z_{x,y}$  is the reference relief,  $z_{x,y}$  is the relief extracted by photometric model. The global results of these measurements are presented in the table 1.

The result obtained by the suggested method is more precise than this obtained by Lambert's model. Consequently, this method is more adapted to the relief extraction of the rough textured reflecting surface.

	Error coefficient
Lambert's model	0.0451
Our method	0.0422

**Table 1.** Comparison of reconstruction errors.

Nevertheless, we can note that the weak difference between the first results presented in table 1 is due to the small size of the specular area comparatively to the global shape.

## 4. CONCLUSIONS AND PERSPECTIVES

In this paper, we first presented how to establish the link between the gray level on image and the relief variations through Lambert's model and the principal 2D numeric integration algorithm. From this classic photometric stereovision technique, we developed a relief extraction method which applies to the rough textured reflecting surface. Thus, in the application of roughness estimation,<sup>14</sup> this method can improve the precision of the estimation of surface roughness.

From this method, it will be possible to exploit a more perfect method of general Lambertian model (Oren-Nayar's model<sup>15</sup>), which takes into account the complex geometric and radiometric phenomena such as masking, shadowing and inter-reflections between facets. This method also allows us to extend our study to dynamic images in the future.

## REFERENCES

1. B. Horn, "Height and gradient from shading," *International Journal of computer vision* **5**, pp. 37–75, august 1990.
2. B. Shahraray and M. Brown, "Robust depth estimation from optical flow," *Second International Conference on Computer Vision, IEEE Comput*, pp. 641–650, December 1988.
3. E. Krotkov, "Focusing," *International Journal of Computer Vision* **1**, pp. 223–237, October 1987.
4. R. Woodham, "Photometric method for determining surface orientation from multiple images," *Optical Engineering* **19**(1), pp. 139–144, 1980.
5. T. Kulick, "Shape from shading using three images," *Computing* **57**(1), pp. 1–24, 1996.
6. B. Kim and R. Park, "Shape from shading and photometric stereo using surface approximation by legendre polynomials," *Computer Vision and Image Understanding* **66**, pp. 255–270, June 1997.
7. R. Zhang and M. Shah, "Iterative shape recovery from multiple images," *Image and Vision Computing* **15**, pp. 801–814, November 1997.
8. K. Torrance and E. Sparrow, "Theory for off-specular reflection from roughened surfaces," *Optical Society of America*, 1967.
9. R. Zhang, P. Tsai, J. Cryer, and M. Shah, "Shape from shading: a survey," *IEEE Transactions on Pattern Analysis and Machine Intelligence* **21**(8), pp. 690–706, 1999.
10. A. Agrawal, R. Raskar, and R. Chellappa, "What is the range of surface reconstructions from a gradient field?," *European Conference on Computer Vision (ECCV)*, 2006.
11. R. Frankot and R. Chellappa, "A method for enforcing integrability in shape from shading algorithms," *IEEE Transactions on Pattern Analysis and Machine Intelligence* **10**, pp. 439–451, july 1988.
12. B.-T. Phong, "Illumination for computer generated images," *Communications of the ACM* **18**(3), pp. 311–317, 1975.
13. J. Blinn, "Models of light reflection for computer synthesized pictures," *Siggraph*, 1977.
14. M. Khoudair, J. Brochard, A. Benslimane, and M.-T. Do, "Estimation of the luminance map for a lambertian photometric model: application to the study of road surface roughness," *Journal of Electronic Imaging* **13**, pp. 515–522, July 2004.
15. M. Oren and S. Nayar, "Generalization of lambert's reflectance model," *Proceedings of the 21st annual conference on Computer graphics and interactive techniques*, pp. 239–246, 1994.